ORIGINAL ARTICLE

The role of transduced bone marrow cells overexpressing BMP-2 in healing critical-sized defects in a mouse femur

M Pensak[1], S Hong[2], A Dukas[1], B Tinsley[1], H Drissi[1], A Tang[3], M Cote[1], O Sugiyama[3], A Lichtler[4], D Rowe[4] and JR Lieberman[3]

The role that transduced mouse bone marrow stromal cells (mBMSCs) engineered to overexpress human bone morphogenetic protein 2 (BMP-2) play in healing critical-sized skeletal defects is largely unknown. We evaluated the interaction between host osteoprogenitor cells and donor mBMSCs transduced with either a lentiviral (LV) vector-expressing red fluorescent protein (RFP) with or without BMP-2 that were implanted into a critical-sized femoral defect. Radiographs taken at the time of killing were evaluated using a five-point scaled scoring system. Frozen histologic sections were analyzed to assess both the transduced cells' role in bone repair and the local osteoprogenitor response. There was complete radiographic bridging in 94% of group I (LV-RFPch-BMP-2-cmyc) and 100% of group III (recombinant human BMP-2) specimens. Radiographs demonstrated a lack of healing in group II (LV-RFPch). Mouse BMSCs transduced with an LV-RFPch-BMP-2 vector were able to induce host cells to differentiate down an osteoblastic lineage and heal a critical-sized defect. However, the donor cells appeared to be functioning as a delivery vehicle of BMP-2 rather than actually differentiating into osteoblasts capable of participating in bone repair as evidenced by a lack of colocalization of the transduced cells to the sites of skeletal repair where the host progenitor cells were found.

INTRODUCTION

The optimal treatment of large bone defects associated with trauma, revision total joint arthroplasty and spinal fusion still has not been identified.[1–3] There is interest in developing regional gene therapy as a potential treatment option because the sustained release of growth factors may enhance bone repair. Both *in vivo* and *ex vivo* strategies have been demonstrated to be successful in healing critical-sized defects in animal studies.[4–11] There is a concern that in a biologically stringent environment there may not be a sufficient number of host cells present at the bone repair site to lead to an adequate biological response with an *in vivo* therapy. Therefore, we have focused on regional gene therapy with an *ex vivo* strategy using a lentiviral (LV) vector containing the complementary DNA (cDNA) for bone morpho-genetic protein 2 (BMP-2). We have been developing gene therapy with a LV vector[9,12] because a prolonged duration of transgene expression is probably necessary to heal the large defects for which gene therapy will be initially used in clinical situations.

One of the critical questions that needs to be answered in an *ex vivo* strategy is what is the role of the transduced cells? Do the transduced bone marrow cells just serve as a delivery vehicle for the growth factor or do they actively participate in bone repair? This information could influence the cell type selected for use in an *ex vivo* strategy. There are a number of candidate cellular delivery vehicles (mesenchymal stem cells from bone marrow, muscle, adipose-derived stem cells and fibroblasts) and all have been successfully used in various preclinical animal models in *ex vivo* regimens.[5,6,12–17] The role of these cells in the bone repair process has not been definitively established.

The purpose of this study was to determine if transduced mouse bone marrow stromal cells (mBMSCs) simply served as a protein delivery vehicle within a critical-sized mouse femoral defect or actively participated in bone repair. We also compared the progenitor cell response with treatment with recombinant human BMP-2 (rhBMP-2) on a collagen sponge versus BMP-expressing bone marrow cells transduced with a LV vector. We hypothesized that donor mBMSCs engineered to express BMP-2 could lead to osteoinduction of host mesenchymal cells and that the donor cells themselves would participate in the bone repair process. By tagging the cells with a unique fluorescent reporter gene, we were able to assess their role in the bone repair process. In addition, by using novel fluorescent reporter mice, we visualized, quantified and compared the osteoprogenitor cell response with BMP expressed by transduced cells and rhBMP-2 protein.

RESULTS

Radiographic assessment of defect healing

Plain radiographic analysis demonstrated that there was complete bridging in 15/16 defects in group I (LV-red fluorescent protein monomeric Cherry (RFPch)-BMP-2) and all the defects in group III (rhBMP-2). None of the specimens in group II (LV-RFPch) demonstrated healing at any time point.

The bone defects in groups I and III that healed had done so by the 14-day time point. The average healing score for group I (LV-RFPch-BMP-2) from 14 days onward, the typical time for bridging to occur, was 4.77 ± 0.46. Fifteen of 16 (94%) specimens at or beyond the 14-day time point had average healing scores of

[1]Department of Orthopaedic Surgery, Orthopaedic Surgery, University of Connecticut Health Center, Farmington, CT, USA; [2]Department of Computer Science and Engineering, University of Connecticut, Storrs, CT, USA; [3]Department of Orthopaedic Surgery, Keck School of Medicine, University of Southern California, Los Angeles, CA, USA and [4]Department of Reconstructive Sciences, University of Connecticut Health Center, Farmington, CT, USA. Correspondence: Dr JR Lieberman, Department of Orthopaedic Surgery, Keck School of Medicine, University of Southern California, 1520 San Pablo Street, Suite 2000, Los Angeles, CA 90033, USA.
E-mail: jay.lieberman@med.usc.edu

5 ± 0.00. The average radiographic healing scores for group III (rhBMP-2) from 14 days and beyond was 5.0 ± 0.00. All 16 of these defects had complete healing (100%). Analysis of the group II (LV-RFPch) specimens revealed an average healing score of 1.39 ± 0.70 across a similar time frame. None of the 16 (0%) specimens at or beyond 14 days had average healing scores of 4 or better. Analysis of variance revealed significant differences among the radiographic scores at 56 days with groups I and III outperforming group II ($P < 0.01$). *Post hoc* testing demonstrated that both the group I ($P < 0.01$) and group III ($P < 0.01$) treatment regimens significantly outperformed group II at all time points from 14 days onward (Figure 1). A weighted kappa value of 0.97 was achieved among the three radiographic reviewers confirming high interobserver reliability.

Frozen histologic analysis

Bone defect healing. We noted two distinct healing responses in the defects. Mice treated with either rhBMP-2 or cells transduced to express BMP-2 (groups I and III) healed the defects through the production of anterior and posterior bony bridges that spanned the critical defect by 14 days. All but one mice in group I formed complete bony bridges at 14 days (15/16) and beyond (one 21-day specimen did not completely bridge). Bridges formed in all specimens (16/16) in rhBMP-2-treated defects (group III). The mode of BMP administration (gene therapy or recombinant protein on a collagen sponge) did not appear to alter the gross healing response. However, the rhBMP-2 in treatment group III elicited a more robust osteoprogenitor response than the transduced cells. In stark contrast, the mice exposed to the RFPch treatment alone (group II) failed to mount any significant healing response and no bony bridge developed (Figure 2).

RFPch expression. In the group I mice, RFPch-positive cells were seen in the defect mainly at the first three time points (7, 14 and 21 days) but the signal was very weak (Figure 2). There did not appear to be any discernible change in the spatial pattern of these cells across the first three time points. In contrast, the mice in group II had a very strong and obvious presence of RFPch-positive cells at the 7- and 14-day time points in the defect (Figures 2 and 3). The cells did appear to be closer to one another and more confined to the region of the defect at 14 days compared with 7 days. By 21 days, the RFPch cells were barely visible in the defect. As expected, we did not see any appreciable RFPch signal in the defect in group III mice (Figure 2).

Histologic evaluation of host and donor cell interactions. Group I mice had a limited presence of GFPemd-positive osteoprogenitor cells in the defect at all time points (Figure 2). In contrast, the mice in group III had a fairly strong presence of GFPemd-positive cells in the defects mainly at 14- and 21-day time points (Figure 2). This may suggest that the BMP released by the cells had a weaker osteoinductive effect than the recombinant protein but the defects still healed in both groups.

In groups I and III, a strong association of the osteoprogenitor cells with the mineralizing anterior and posterior bony bridges could be seen at 14 days and 21 days (Figure 2). These findings suggest that the host cells were recruited to the vicinity of the defect by the potent osteoinductivity of BMP. There was a less robust response in group I versus group III (Figure 2).

By 56 days, the bony bridges had markedly thinned out and a very faint population of Col2.3GFPemd activity could be detected along the inner margin of the bone bridge. No newly mineralized bone could be detected at this final time point.
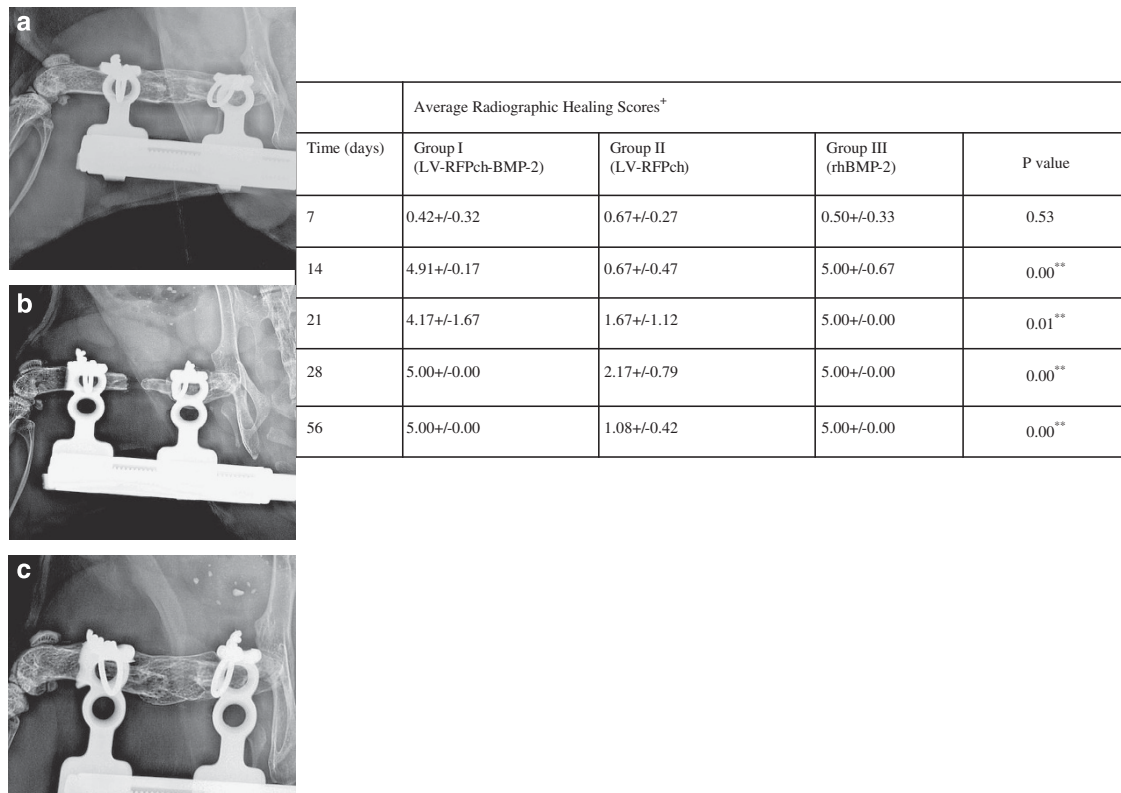

	Average Radiographic Healing Scores[+]			
Time (days)	Group I (LV-RFPch-BMP-2)	Group II (LV-RFPch)	Group III (rhBMP-2)	P value
7	0.42+/-0.32	0.67+/-0.27	0.50+/-0.33	0.53
14	4.91+/-0.17	0.67+/-0.47	5.00+/-0.67	0.00[**]
21	4.17+/-1.67	1.67+/-1.12	5.00+/-0.00	0.01[**]
28	5.00+/-0.00	2.17+/-0.79	5.00+/-0.00	0.00[**]
56	5.00+/-0.00	1.08+/-0.42	5.00+/-0.00	0.00[**]

Figure 1. Representative X-rays of (**a**) group I, (**b**) group II and (**c**) group III mouse defects at 56 days showing complete bridging of specimens in groups I and III in contradistinction to group II, which failed to bridge the defect. Statistically significant higher radiographic healing scores were noted in groups I and III at all times points from 14 days and onward compared with group II. [+]Radiographic scores are given as the mean ± s.d. **Statistically significant differences between groups I and III compared with group II.
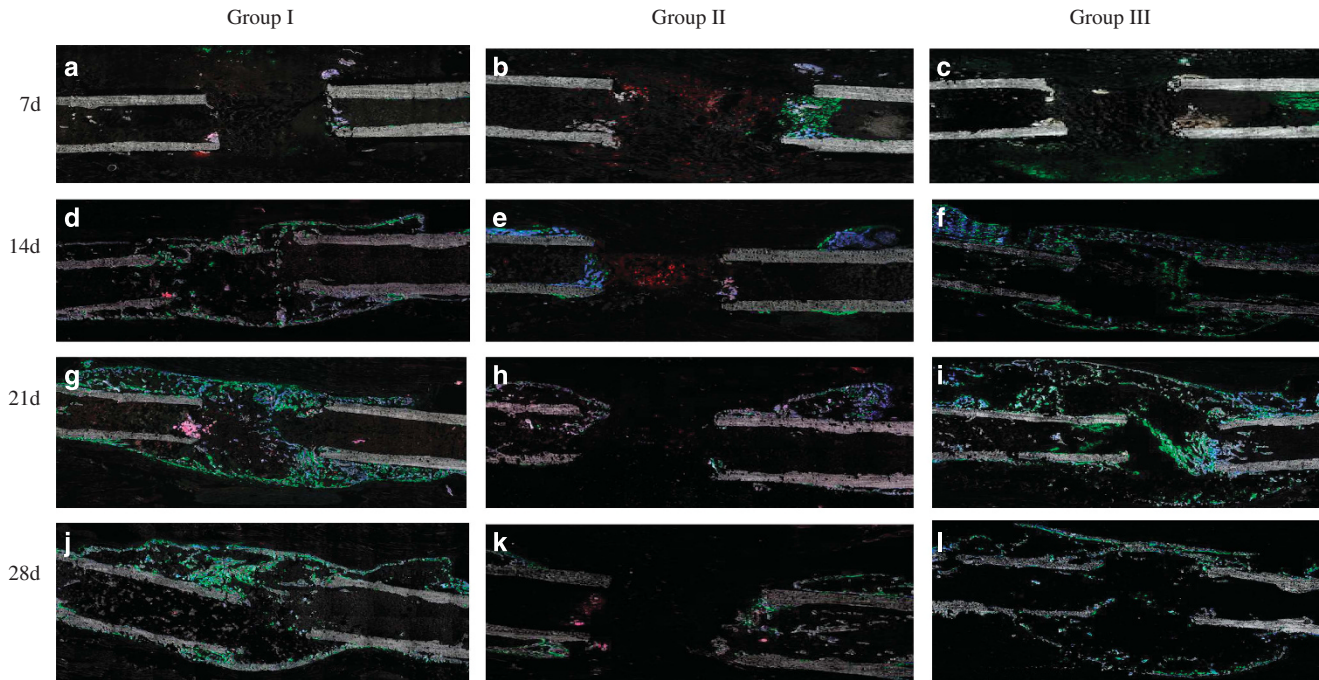
Figure 2. Representative 2 mm defects (magnification x10) at 7, 14, 21 and 28 days post-op from Col2.3GFPemd transgenic mice treated with either mBMSCs expressing RFPch-BMP-2 (**a**, **d**, **g**, **j**), RFPch (**b**, **e**, **h**, **k**) or an absorbable collagen sponge loaded with 5 mcg of rhBMP-2 (**c**, **f**, **i**, **l**). The RFPch signal in the group II mice was much stronger at the first two time points compared with group I. In addition, the donor cells appeared to condense and coalesce within the defect over the course of the first 2 weeks. The RFPch signal was very weak by 21 and 28 days in group II. No healing of the defects was appreciated in the group II specimens. In both of the BMP-2 treatment arms, the defects were bridged by 14 days. A very small amount of red donor cells expressing RFPch-BMP-2 can be seen within the region of the defects in the group I specimens at all time points, though they were most visible at 7 and 14 days. As expected, no red signal is appreciated in the group III specimens as there were no transduced cells implanted into these defects. Green color represents host Col2.3GFPemd-positive osteoprogenitor cells and blue represents newly mineralized bone stained with tetracycline. Notably, no significant colocalization of red and green cells are appreciated in the group I specimens.
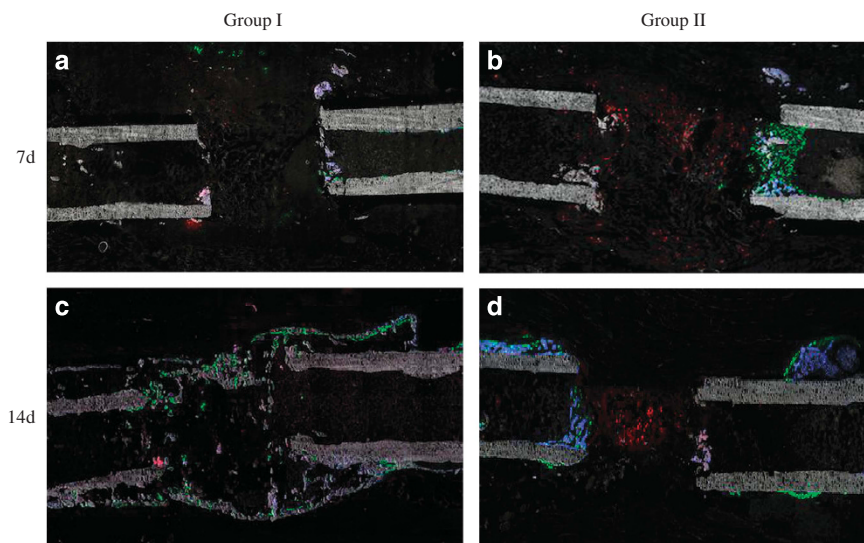

Figure 3. Defect region (magnification x25) at 7 and 14 days post-op from Col2.3GFPemd transgenic mice treated with mBMSCs expressing RFPch-BMP-2 (**a, c**) or RFPch (**b, d**). In the group I specimens, the donor cells had a very weak expression of the RFPch protein at both time points though the signal was clearly more visible at 7 days. In contrast, the group II specimens displayed a very strong RFPch signal at both early time points with the cells coalescing and condensing into the region of the defect from 7 days to 14 days. Green color represents host Col2.3GFPemd-positive osteoprogenitor cells and blue represents newly mineralized bone stained with tetracycline.

The group II mice had no visible Col2.3GFPemd activity in the defect at all time points (Figures 2 and 3). However, in the region of the external fixator both Col2.3GFPemd-positive cells and newly mineralized bone could be seen by 14 days, which may have resulted from periosteal reaction (Figure 2).

Very few RFPch-positive cells were present in the vicinity of the bone bridges and they did not appear to be colocalizing with the host green cells in group I mice (Figure 2). These findings suggest that the donor cells induced the host cells' development into an osteoblastic lineage but did not directly participate in skeletal

Table 1. Defect parameters measured at 7,14, 21, 28 and 56 days

Time point (days)	Group I: LV-RFPch-BMP-2	Group II: LV-RFPch	Group III: RhBMP-2
RFPch+ cell/TV defect			
7	0.31 ± 0.43‡	1.07 ± 0.12†	0.1 ± 0.21‡
14	0.77 ± 1.14	1.48 ± 0.55†	0.26 ± 0.51
21	0.46 ± 0.75	0.12 ± 0.05	0 ± 0
28	0.24 ± 0.23	0.2 ± 0.32	0.41 ± 0.8
56	0.03 ± 0.04	0.07 ± 0.09	0 ± 0
RFPch+ cell/bone surface defect			
7	15.13 ± 16.66	5.41 ± 2.79	5.56 ± 11.11
14	14.29 ± 17.6	16.53 ± 9.26*	4.98 ± 9.9
21	9.62 ± 16.99	3.39 ± 2.7	0 ± 0
28	4.78 ± 5.53	1.37 ± 1.45	6.41 ± 12.27
56	0 ± 0	0.15 ± 0.29	0 ± 0
GFPemd+cell/TV defect			
7	0.07 ± 0.09	009 ± 0.19	0.04 ± 0.05
14	0.44 ± 0.47	0.19 ± 0.17	2.28 ± 2.22
21	0.37 ± 0.52	0.2 ± 0.14	2.93 ± 4.21
28	0.36 ± 0.31	0.12 ± 0.08§	1.07 ± 0.65‡
56	0.06 ± 0.05	0.38 ± 0.3	0.09 ± 0.1
LabelGFPemd+cell/bone surface defect			
7	0.66 ± 0.74	1.33 ± 2.67	0.15 ± 0.31
14	4.02 ± 3.96	2.02 ± 2.8	2.63 ± 3.72
21	4.51 ± 6.59	2.31 ± 2.83	11.46 ± 11.9
28	2.33 ± 1.57§	0.33 ± 0.26§	10.53 ± 2.79
56	0.67 ± 0.79	5.55 ± 7.19	0.67 ± 0.77

Abbreviations: BMP-2, bone morphogenetic protein-2; LV, lentiviral; RhBMP-2, recombinant human BMP-2; RFPch, red fluorescent protein monomeric Cherry; TV, total volume. Data expressed as mean ± s.d. *$P < 0.05$ compared with all other time points in the same group. †$P < 0.05$ compared with days 21, 28, and 56. ‡$P < 0.05$ compared with LV-RFPch. §$P < 0.05$ compared with RhBMP-2.

Table 2. Bone bridge parameters measured at 7, 14, 21, 28 and 56 days

Time point (days)	Group I: LV-RFPch-BMP-2	Group III: RhBMP-2
GFPemd+cell/bone surface anterior bone bridge		
7	0.12 ± 0.25	0 ± 0
14	24.97 ± 20.34	29.82 ± 17.65†
21	13.4 ± 10.5	19.55 ± 15.38
28	21.02 ± 16.02	25 ± 4.49
56	23.16 ± 9.58	12.23 ± 9.38
GFPemd+cell/bone surface posterior bone bridge		
7	4.09 ± 7.15	2.17 ± 4.13
14	23.78 ± 20.65	26.84 ± 12.12†
21	14.44 ± 9.16	15 ± 11.23
28	14.35 ± 12.91	21.68 ± 13.26
56	16.1 ± 6.2	7.91 ± 5.96
BV/TV anterior bone bridge		
7	1.13 ± 1.36	0.6 ± 0.72*
14	16.68 ± 6.53	23.07 ± 7.78
21	12.34 ± 5.81	18.6 ± 5.62
28	17.59 ± 9.11†	19.83 ± 5.09
56	40.07 ± 8.43*	31.2 ± 10.02
BV/TV posterior bone bridge		
7	0.65 ± 0.33	0.24 ± 0.12
14	16.56 ± 9.19	16.62 ± 6.95
21	20.07 ± 22.73	11.18 ± 4.95
28	9.47 ± 11.01	12.91 ± 14.65
56	32.47 ± 18.34	28.64 ± 10.22†

Abbreviations: BMP-2, bone morphogenetic protein-2; BV, bone volume; GFP, green fluorescent protein; LV, lentiviral; RhBMP-2, recombinant human BMP-2; RFPch, red fluorescent protein monomeric Cherry; TV, total volume. Data expressed as mean ± s.d. *$P < 0.05$ compared with all other time points in the same group. †$P < 0.05$ compared with day 7.

repair. As expected, no colocalization of red and green cells could be detected in the defect or bony bridges in the group III mice (Figure 2).

The group II defects were devoid of osteoprogenitor cells and failed to form bony bridges supporting the notion that the RFPch donor mBMSCs did not possess the osteoinductive capacity to recruit host osteoprogenitor cells (Figures 2 and 3). Histomorphometric parameters that were designed to detect for colocalization of red and green cells within the defect did not reveal any significant results across time points.

Histomorphometric quantitation of osteoprogenitor cell recruitment in the bone defect

In the group I mice, we found no significant temporal differences in any of the histomorphometric parameters in the region of the bone defect. In the group II mice, we detected a significant temporal difference in the RFPch+cell/total volume (TV) parameter. Mirroring our histologic observations, the parameters were significantly larger at 7 and 14 days compared with all other time points (Table 1). In addition, the percentage of RFPch-positive cells associated with the bone surfaces (RFPch+cell/bone surface) peaked at 14 days and was significantly larger compared with all other time points (7 days, $P = 0.034$; 21 days, $P = 0.010$; 28 days, $P < 0.01$ and 56 days, $P < 0.01$) (Table 1). The GFPemd+cell/TV parameter, which quantifies the ratio of GFPemd-positive cells as a percentage of the defect volume was nearly 5x–7x smaller in group I than that seen in our positive control, group III, at 14 and 21 days (Table 1). This suggests that in this model rhBMP was

more efficacious at recruiting osteoprogenitor cells when delivered on a collagen sponge compared with cell-based delivery.

Comparison across treatment groups at a given time point revealed significant differences among some of the cellular parameters. At 7 days, we noted a larger RFPch+cell/TV parameter in group II compared with group I ($P < 0.01$) and III ($P < 0.01$) (Table 1) suggesting that the LV-RFPch vector induced a stronger expression of RFPch than the LV-RFPch-BMP-2 vector. At 28 days, there were differences in the GFPemd+cell/TV parameter among the treatment groups ($P = 0.0275$). *Post hoc* testing revealed that the difference between groups II and III was significant in favor of group III (Table 1). In addition, newly mineralized bone and Col2.3GFPemd cells were found to colocalize along the bone surfaces in greater quantities in group III compared with both groups I ($P < 0.01$) and II ($P < 0.01$). This was expressed via the LabelGFPemd+cell/bone surface parameter (Table 1).

Histomorphometric quantitation of osteoprogenitor cell recruitment in the healing bone

The area within the perimeter of the anterior and posterior bone bridges was analyzed to determine if and how the host and donor cells were interacting to effect skeletal repair. There were no differences among any of the cell-based histomorphometric parameters in the group I mice across time points (Table 2). However, with respect to the anterior bone bridge, the bone volume (BV)/TV value at 28 days was significantly greater than at 7 days and the 56-day value was significantly greater than all other time points (Table 2). The group III mice had significantly larger GFPemd+cell/bone surface values at 14 days compared with 7 days ($P = 0.022$ anterior, $P = 0.033$ posterior) in both the

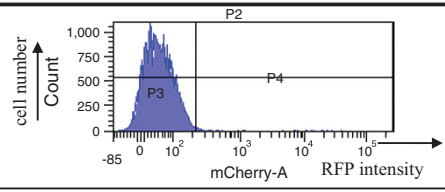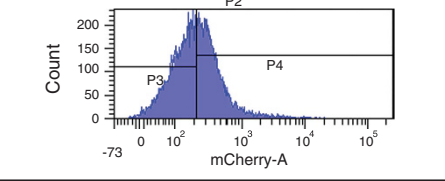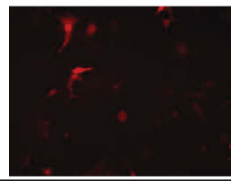## FACS analysis of RFP cherry expression
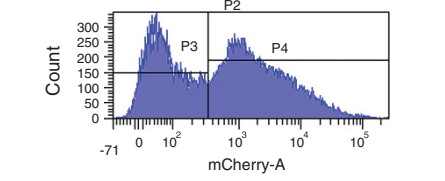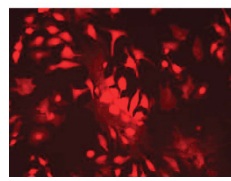
mBMSCs	histogram		%positive	MFI	microscope
Non-transduced			0.5%	59	
LV-RFPch-BMP-2-cmyc day 2			47.7%	325	
LV-RFPch-BMP-2-cmyc day 6			57.9%	3193	

Figure 4. Flow cytometric analysis of RFP monomeric cherry expression in cells. The expression was detected in 47.4% of the transduced cells at day 2 and 57.9% at day 6 after transduction with LV-RFPch-BMP-2-cmyc at m.o.i of 25.

anterior and posterior bridges (Table 2). In group III, all time points that had a bony bridge form (14 days and beyond) showed significantly larger BV/TV values compared with the day 7 value with respect to the anterior bone bridge only. In the posterior bone bridge, the BV/TV value at 56 days was significantly greater than the 7-day time point only (Table 2).

Fluorescence-activated cell sorting analysis and *in vitro* BMP-2 enzyme-linked immunosorbent assay

After its development, the efficacy of the LV-RFPch-BMP-2-cmyc viral vector was qualitatively assessed using fluorescence-activated cell sorting analysis to analyze the RFP monomeric cherry expression in cells. The expression was detected in 47.4% of the transduced cells at day 2 and 57.9% of the cells 6 days after transduction with LV-RFPch-BMP-2-cmyc at multiplicity of infection (m.o.i) of 25 (see Figure 4).

In vitro BMP-2 production by mBMSCs transduced with LV-RFPch-BMP-2-cmyc was measured using enzyme-linked immunosorbent assay. At m.o.i of 50, the 1×10^5 cells transduced with LV-RFPch-BMP-2-cmyc produced 0.39 ± 0.05 ng of BMP-2 in a 24-h period. The m.o.i of 50 was chosen to maximize our BMP-2 production as m.o.i's of 75 and 100 were too toxic to the cells. Non-transduced and LV-RFPch transduced cells were used as negative controls and produced significantly less BMP-2 (0.04 ± 0.02 ng and 0.02 ± 0.02 ng, respectively; see Figure 5).

DISCUSSION

In this study, we demonstrated that BMP-2 loaded on a collagen sponge or delivered by mBMSCs transduced with a LV vector induces healing of a critical-sized femoral defect in a mouse by 14 days after implantation. Skeletal repair appeared to be accomplished via induction of the host Col2.3GFPemd progenitor cells in both groups. We did not observe any significant colocalization of the host and donor cells in group I mice suggesting that the transduced cells were delivery vehicles of BMP-2. The transduced donor cells appeared to recruit host
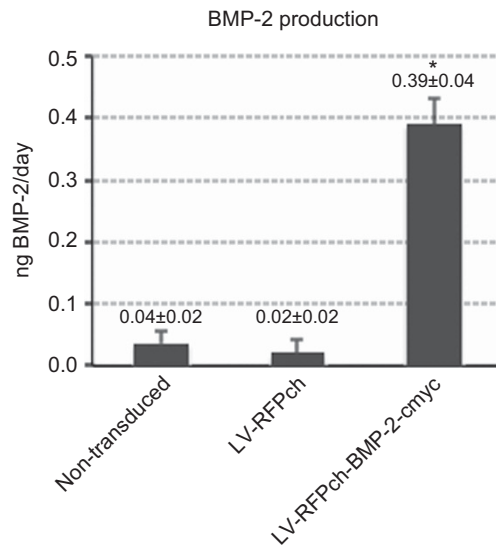

Figure 5. *In vitro* BMP-2 production by mBMSCs transduced with LV-RFPch-BMP-2-cmyc (1×10^5 cells). The 1×10^5 cells transduced with LV-RFPch-BMP-2-cmyc produced 0.39 ± 0.05 ng of BMP-2 in 24 h when m.o.i was 50. Non-transduced and LV-RFPch transduced cells were used as negative controls. (1) Non-transduced. (2) LV-RFPch (m.o.i = 50). (3) LV-RFPch-BMP-2-cmyc (m.o.i = 50). *$P < 0.05$ compared with non-transduced cells.

osteoprogenitor cells in a paracrine manner, causing them to migrate into and around the bone defect, but did not seem to induce the transduced cells themselves into functional osteoblasts.

Both treatment groups I and II had RFPch-positive cells that were mainly seen in the defect at 7 and 14 days. However, the RFPch signal and cell population was considerably more robust in group II mice compared with group I at these two early time

Structure of LV-RFPch-BMP-2-cmyc vector

| Chimeric LTR | Ψ | RRE | | cppt | | RhMLV promoter | RFPch | T2A | BMP2cmyc | | Chimeric LTR |

LTR: long terminal repeat   Ψ: packaging signal
RRE: Rev-responsible element   cppt: central polyprine tract
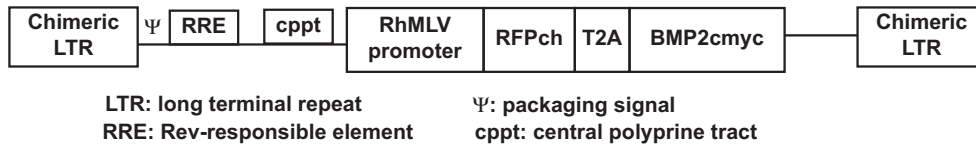
Figure 6. Structure of the dual gene expression LV vector to overexpress RFP monomeric cherry and c-myc epitope-tagged BMP-2 genes.

points. This discrepancy in RFPch expression may have also translated into weaker than usual BMP-2 expression in the LV-RFPch-BMP-2 treatment group perhaps blunting both the paracrine and autocrine signaling potential of the donor cells in that treatment group. We speculate that this was directly attributable to our vector construct, which used a single promoter to drive the translation of two separate protein products. However, the defects still healed suggesting that the progenitor response is influenced by the quantity, kinetics and duration of BMP release.

The progenitor cell response to the rhBMP-2 was more robust than that seen with the transduced bone marrow cells yet the defects healed in both groups. This finding may be related to the kinetics of BMP release with the collagen sponge compared with transduced cells. There is a fairly rapid release of BMP from the collagen sponge over the first day, which is associated with an early osteoprogenitor response.[18] The transduced cells probably released the BMP at a steadier rate producing a sufficient osteoprogenitor response to heal the defect. In a prior study, we noted that rat bone marrow cells transduced with a LV vector containing the cDNA for BMP-2 produced better quality bone in the defect than cells transduced with a BMP-2 containing adenoviral vector although the adenoviral vector produced approximately three times as much BMP.[12] We hypothesized that the longer duration of BMP production associated with the LV vector was responsible for the better quality of the bone repair.[12,19,20]

The role of the transduced cells in the bone repair process may influence the cellular delivery vehicle that is chosen in an ex vivo strategy. When treating large bone defects it may be important to select a specific cell type (bone marrow, muscle, adipose-derived stem cells, fibroblasts) that is associated with a significant amount of BMP production and a vector that produces the protein for a prolonged period of time. Lee et al.[14] used a Y-chromosome-specific technique of fluorescent in situ hybridization to track male muscle-derived cells transduced with an adenovirus-BMP-2 vector and implanted them into a female SCID mouse calvarial defect. Y-chromosome bearing cells were detected on the newly formed bone surfaces and stained positive for osteocalcin suggesting that they differentiated down an osteogenic lineage. However, calvarial defects heal by intramembranous ossification. The femoral defect healing noted with BMP-producing cells placed in a defect stabilized with an external fixator includes a combination of endochondral ossification and intramembranous ossification.

Utilizing an ex vivo gene approach, Gamradt et al.[21] transduced rat bone marrow cells with an adenoviral-BMP-2-myc vector and implanted them in a SCID mouse radial defect. The investigators found that the cells were able to participate in bone repair by differentiation into osteocyte-like cells. Peak BMP-2 production took place between 7 and 14 days, which was similar to the profile of RFPch expression seen in both of the gene therapy treatment groups in our study. Gazit et al.[22] implanted mesenchymal stem cells engineered to express rhBMP-2 and the lac-Z gene into a SCID mouse radial defect. The engrafted cells developed into osteoblasts and expressed both rhBMP and beta-gal while significantly enhancing bone repair at 4 and 8 weeks after implantation. However, in both of these studies the defects were

not stabilized with fixation devices, therefore, the healing cascade is different than with the more rigid stabilization obtained with an external fixator. As the radial defect model does not include bone fixation, it does not simulate the clinical scenario where gene therapy will be utilized.

The findings of this study have important implications for the development of gene therapy strategies for use in patients. It appears that the quantity of BMP produced by various types of candidate human cell delivery vehicles (that is, bone marrow-derived stem cells, adipose-derived stem cells and muscle-derived stem cells) influences the quality of the bone repair in critical-sized bone defect models. We have developed an ex vivo strategy because it allows us to select the cells that are transduced with the LV vector. This may be advantageous when treating large bone defects compared with an in vivo strategy, which requires a donor cell population to respond to local growth factor delivery. It should be noted that Schwarz et al. circumvented many of the shortcomings associated with in vivo gene therapy by coating structural allografts with rAAV expressing the constitutively active BMP type 1 receptor Alk2 (caAlk2), VEGF and RANKL.[23,24] This novel strategy uses allograft bone to deliver growth factors and serve as a scaffold for bone repair. This construct induced formation of a bony mineralized callus and the recruitment of angiogenic cells and facilitated osteoclasts to remodel allografts when implanted into mouse femoral defects.[23,24] Interestingly, the results of this study support our findings using an ex vivo strategy that an exogenous growth factor needs to be delivered over time to induce optimal bone healing.

There are some limitations to this study. First, we cannot definitively state the donor cells did not participate at all in the bone repair process. However, it appears that the critical element to promote bone repair is the production of BMP. This finding may influence the selection of cell type when developing an ex vivo strategy. Second, the healing was quite prominent by 14 days in the two BMP-2 treatment groups. It is possible that there may have been a time point in between days 0 and 14 in which the RFPch signal peaked in group I. Once the bone healing occurs it may be more difficult to detect the transduced cells in the defect. Regardless, the histologic analysis strongly suggests that most of the cellular interactions between the host and donor cells in this model happens in the first 2 weeks after implantation with a less robust response taking place for an additional 2 weeks out until the 4-week mark. Finally, we evaluated a critical-sized defect that was stabilized by an external fixator. In this model, the bone defect is healed by 14–21 days. The role of the transduced cells in the healing process may be influenced by the rigidity of the fixation used.

In summary, mBMSCs transduced with an LV-RFPch-BMP-2 vector in an ex vivo manner were able to induce host osteoprogenitor cells to differentiate down an osteoblastic lineage and induce bony bridging of a critical-sized mouse femoral defect. However, the donor cells appeared to be functioning more as a BMP delivery vehicle than actually differentiating into osteoblasts capable of participating in the bone repair process. Healing of the bone defect occurred with treatment with both BMP-producing transduced bone marrow cells and with rhBMP-2. Given that the early osteoprogenitor response to rhBMP-2 was more robust but

the defects healed in both groups both the kinetics and duration of BMP release at the bone repair site need to be optimized to maximize the bone repair.

MATERIALS AND METHODS

Construction of LV vectors

A plasmid of a bicistronic LV vector (pLV-RFPch-BMP-2-cmyc) was constructed for gene expression of an RFPch coding sequence[25,26] and a cmyc epitope-tagged BMP-2 gene (BMP-2-cmyc) (see Figure 6). The RFPch and BMP-2-cmyc cDNAs were connected by T2A sequence during overlap extension PCR procedure.[27] In the first PCR, RFPch-T2A was amplified by PCR using Phusion High-Fidelity DNA Polymerase (New England Biolabs, Ipswich, MA, USA) using RFPch-forward primer including BamHI site (5'-CGCGGATCCGCCACCATGGTGAGCAAG-3'), T2A-reverse primer (5'-AGGG CCGGGATTCTCCTCCACGTCA-3') and pCDH-EF1a-RFPch-T2A-Puro plasmid as a template. T2A-BMP-2-myc was amplified using BMP-2-myc-forward primer including T2A sequence at 5' end (5'-GAGGGCAGAGGAA GTCTTCTAACATGCGGTGACGTGGAGGAGAATCCCGGCCCTATGGTGGCCGGG ACCCGCTG-3'), BMP-2-myc-reverse primer including SalI site (5'-CCGGTCG ACCTAGCGACACCCACAACCCT-3') and pACCMVpL-pASBMP-2[Myc] plasmid[21] for a template. These PCR products were run on an agarose gel and purified by QIAEX II Gel Extraction Kit (QIAGEN, Valencia, CA, USA). In the second PCR step, purified amplicons of RFPch-T2A and T2A-BMP-2-cmyc served as template DNAs. The RFPch-forward primer and the BMP-2-cmyc-reverse primer were used to create the full-length RFPch-BMP-2-cmyc linked by T2A.

The final PCR amplicon was cloned into a commercial T-vector: pGEM-T Easy Vector (Promega, Madison, WI, USA) after 3' A overhang addition. No mutation and no frame shift were confirmed in amplified RFPch-BMP-2-cmyc by sequencing analysis (DNA sequencing service, Genewiz, South Plainfield, NJ, USA). RFPch-BMP-2-cmyc cDNA fragment was isolated by BamHI and SalI restriction enzymes from the T-vector. The pLV-RFPch-BMP-2-cmyc plasmid was created by replacement of GFPemd gene with RFPch-BMP-2-cmyc in the LV backbone plasmid SIN18-RhMLV-E plasmid.[28,29]

A plasmid of a control vector was also created for single gene expression of RFP (without BMP-2-cmyc). RFPch cDNA was amplified by PCR using the RFPch-forward primer and an RFP-reverse primer containing SalI site (5'-TTGGTCGACCTACTTGTACAGCTCGTCCAT-3'). The PCR amplicon was cloned into pGEM-T Easy Vector, then transferred to the LV backbone plasmid (pLV-RFPch).

Cell culture and transduction with LV vector

mBMSCs were obtained from the femurs and tibias of 8-week-old male BL/6 mice. Whole bone marrow contents were suspended with Iscove's modified Dulbecco's media (Life Technologies, Grand Island, NY, USA) supplemented 15% fetal bovine serum (Omega Scientific, Tarzana, CA, USA), penicillin (100 U ml^{-1}) and streptomycin (100 mg ml^{-1}), and plated on a 10-cm dish. The adherent mBMSCs were cultured for 4–5 days before first passage and non-adherent cells were removed by changing media. Adherent mBMSCs were plated 1×10^5 cells per six-well plate or 1×10^6 cells per 10-cm dish on the day before viral transduction.

The mBMSCs were transduced with the LV vector at m.o.i of 50 overnight (18–20 h). Transduction was carried out in 5-ml media containing 0.8 μg ml^{-1} polybrene (Sigma, St Louis, MO, USA). The media including the viral vector was replaced with 10 ml of fresh media after transduction.

In vitro BMP-2 quantification

LV transduced mBMSCs (1×10^5 cells) were incubated for another 24 h from the end of transduction. The culture media of transduced cells was collected for analysis of in vitro BMP-2 production. The BMP-2 amount during a 24-h period was quantified by enzyme-linked immunosorbent assay kit (Quantikine, R&D Systems, Minneapolis, MN, USA) according to the manufacturer's instructions. The enzyme-linked immunosorbent assay result showed the BMP-2 amount (ng BMP-2 per day), which was produced by 1×10^5 cells (Figure 5).

Flow cytometric analysis of RFPch expression

The RFP expression was evaluated in pLV-RFPch-BMP-2-cmyc-transduced mBMSCs at 7 days after transduction. The transduced cells (1×10^6) were harvested by trypsinization and analyzed via a BD LSR II flow cytometer (BD Biosciences, San Jose, CA, USA). The percentage of RFPch-positive cells

and the mean fluorescent intensity of RFPch expression were analyzed by FACSDiva version 6.1.1 software (BD Biosciences). The visualized RFPch expression of the cells was also detected under a fluorescence microscope (Figure 4).

Animal studies

All animal studies were performed after approval by the Animal Care Committee at our institution. Critical sized mid-diaphyseal femoral defects (2mm) were created in 4- to 5-month-old male BL/6 lineage-specific transgenic mice expressing Col2.3GFPemerald (GFPemd) and stabilized with an external fixator according to a previously published technique.[30]

There were three study groups: group I, 3 million mBMSCs transduced with LV-RFPch-BMP-2-cmyc, group II (negative control group), 3 million (mBMSCs) transduced with LV-RFPch and group III, 5 mcg rhBMP-2 loaded on absorbable collagen sponge (Medtronic, Minneapolis, MN, USA)).

Mice were killed and analyzed at 7,14, 21, 28 and 56 days. There were four mice per time point. One day before killing, a weight-based dose of demeclocycline (50 mg kg^{-1}, concentration 12.5 mg ml^{-1}) was injected intraperitoneally to demonstrate the areas of the new bone formation.

Radiographic evaluation

Radiographs of the operated limbs were obtained at each time point up until killing. Final radiographs were assessed by three observers and defect healing was scored from 0 to 5 based on a previously published protocol.[4] A score of 0 was given if there was no healing, 0–25% healing was given 1, 25–50% was 2, 50–75% was 3, 75–99% was 4 and complete healing was 5. A weighted kappa value was calculated to determine the interobserver reliability among the radiographic reviewers.

Non-decalcified, frozen histology

At the time of killing, the operated legs were harvested, fixators removed and samples were assessed using a previously established non-decalcified fluorescent histology protocol.[31] Sagittal cryosections (5 μm) through the non-decalcified bone were made using a Leica CM3050S cryostat (Leica, Wetzlar, Germany). Cryosections were transferred onto a special tape (Cryofilm Type2C, Section-lab, Hiroshima, Japan) and stored at − 20 °C until imaging.

Fluorescent imaging

Frozen sections were imaged using a Zeiss Imager Z1 microscope (Carl Zeiss, Thornwood, NY, USA) and analyzed with Axio Vision Rel.4.7 software (Carl Zeiss). Fluorescent filters (Chroma Technology, Bellows Falls, VT, USA) captured separate images based on the fluorescent colors of the slide being analyzed according to a previously established protocol.[31,32] Tetracycline, Col2.3GFPemd and RFPcherry were imaged with separate fluorescent filters: (GFPemd with a green filter (cat.#51019), RFPcherry with a red filter (cat.#31002) and tetracycline with a yellow filter (Chroma Technology Custom HQ409sp, 425dcxr,HQ555/30, set lot C-104285)). A differential interference contrast image was acquired at the same time as the endogenous fluorescence imaging. A final composite image consisting of the individual fluorescent signals and the differential interference contrast image was obtained and converted to a JPEG file for further analysis.
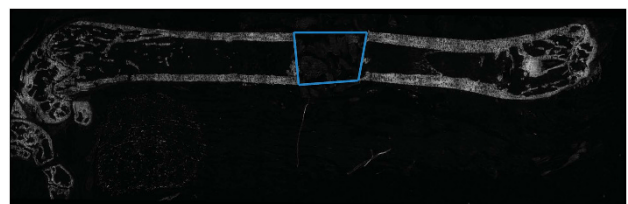

Figure 7. Outline of the region of interest for histomorphometric evaluation of group II specimens (LV-RFPch), which failed to heal the critical-sized defect.
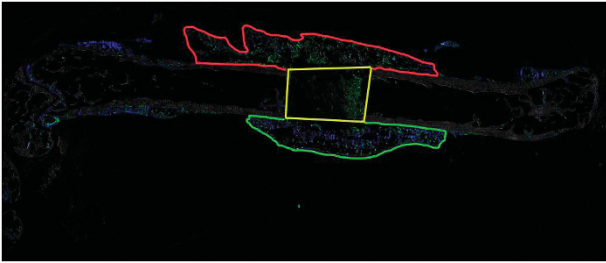
Figure 8. Schematic outline of the regions of interest for histo morphometric evaluation of group I (LV-RFPch-BMP-2) and group III (rhBMP-2) specimens, which healed the critical-sized defect by formation of an anterior and posterior bony bridge.

Histomorphometric analysis of the green fluorescent protein (GFP) expression

There were two patterns of healing noted across the three treatment groups. Accordingly, the regions of interest (ROIs) for analysis of GFP expression and mineral label were different for group II (no bridging of defect observed) compared with groups I and III (bridging of defect observed). The defect was chosen as the ROI for the group II mice (Figure 7). The defect, upper and lower bone bridges were chosen as the regions of interest for groups I and III (Figure 8). As the bony bridges did not appear before day 14 in BMP-treated samples (groups I and III), only the defect ROI was analyzed at the 7-day time point. The ROIs were created on top of the final composite JPEG image using Adobe Photoshop software. Three volume ratios were measured as well as a novel parameter that attempted to quantify the interaction between the host's green cells, donor red cells and newly mineralized bone. According to a previously published protocol[33], quantification within an ROI was done using computer-automated bone histomorphometric techniques introduced by Hong et al.[34,35] following the standardized nomenclatures.[36]

Bone and GFP signals underwent separate segmentation according to Otsu's thresholding method.[37] Otsu's method is based on the histogram of the gray intensities of the signal and provides a threshold that separates grayscale pixels into black and white signal groups. The ratio of GFP-positive cell volume or BV over the TV of the ROI represents a volume ratio. A computer algorithm in Matlab software (Natick, MA, USA) counts the number of white pixels in the segmented (black and white) image that is obtained from the grayscale GFP signal channel to determine the area of the GFP-positive cells. Measured volume ratios are (1) BV/TV; (2) Cell (cell volume)/TV; and (3) Cell (cell volume)/BV. Cell/BV is calculated by dividing Cell/TV by BV/TV. A surface ratio, LabelGFPemd+cellRFPch+cell/bone surface, was calculated to see how host and donor cells interacted with one another in areas of newly mineralized bone.

Statistical analysis

Descriptive statistics to characterize the study groups were reported using mean and s.d. where appropriate. The weighted kappa statistic was calculated to examine the inter-rater reliability of the radiographic grading scheme. Comparisons between groups at study time points as well as comparisons within each group across time points were analyzed with one-way analysis of variance. When significant, post hoc pair wise comparisons were conducted using the Sidak method. An alpha level of 0.05 was considered significant for all analyses. All statistical analysis was performed using Stata 12 (StataCorp. 2011. Stata Statistical Software: Release 12. College Station, TX, USA: StataCorp LP).

CONFLICT OF INTEREST

The authors declare no conflict of interest.

REFERENCES

1 Silber JS, Anderson DG, Daffner SD, Brislin BT, Leland JM, Hilibrand AS et al. Donor site morbidity after anterior iliac crest bone harvest for single-level anterior cervical discectomy and fusion. Spine (Phila PA 1976) 2003; **28**: 134–139.

2 Younger EM, Chapman MW. Morbidity at bone graft donor sites. J Orthop Trauma 1989; **3**: 192–195.

3 Mastrogiacomo M, Muraglia A, Komlev V, Peyrin F, Rustichelli F, Crovace A et al. Tissue engineering of bone: search for a better scaffold. Orthod Craniofac Res 2005; **8**: 277–284.

4 Lieberman JR, Daluiski A, Stevenson S, Wu L, McAllister P, Lee YP et al. The effect of regional gene therapy with bone morphogenetic protein-2-producing bone-marrow cells on the repair of segmental femoral defects in rats. J Bone Joint Surg Am 1999; **81**: 905–917.

5 Park J, Ries J, Gelse K, Kloss F, von der Mark K, Wiltfang J et al. Bone regeneration in critical size defects by cell-mediated BMP-2 gene transfer: a comparison of adenoviral vectors and liposomes. Gene Therapy 2003; **10**: 1089–1098.

6 Shen HC, Peng H, Usas A, Gearhart B, Fu FH, Huard J. Structural and functional healing of critical-size segmental bone defects by transduced muscle-derived cells expressing BMP4. J Gene Med 2004; **6**: 984–991.

7 Hsu WK, Sugiyama O, Park SH, Conduah A, Feeley BT, Liu NQ et al. Lentiviral-mediated BMP-2 gene transfer enhances healing of segmental femoral defects in rats. Bone 2007; **40**: 931–938.

8 Peterson B, Zhang J, Iglesias R, Kabo M, Hedrick M, Benhaim P et al. Healing of critically sized femoral defects, using genetically modified mesenchymal stem cells from human adipose tissue. Tissue Eng 2005; **11**: 120–129.

9 Virk MS, Sugiyama O, Park SH, Gambhir SS, Adams DJ, Drissi H et al. 'Same day' ex-vivo regional gene therapy: a novel strategy to enhance bone repair. Mol Ther 2011; **19**: 960–968.

10 Bertone AL, Pittman DD, Bouxsein ML, Li J, Clancy B, Seeherman HJ. Adenoviral-mediated transfer of human BMP-6 gene accelerates healing in a rabbit ulnar osteotomy model. J Orthop Res 2004; **22**: 1261–1270.

11 Baltzer AW, Lattermann C, Whalen JD, Wooley P, Weiss K, Grimm M et al. Genetic enhancement of fracture repair: healing of an experimental segmental defect by adenoviral transfer of the BMP-2 gene. Gene Therapy 2000; **7**: 734–739.

12 Virk MS, Conduah A, Park SH, Liu N, Sugiyama O, Cuomo A et al. Influence of short-term adenoviral vector and prolonged lentiviral vector mediated bone morphogenetic protein-2 expression on the quality of bone repair in a rat femoral defect model. Bone 2008; **42**: 921–931.

13 Evans CH, Liu FJ, Glatt V, Hoyland JA, Kirker-Head C, Walsh A et al. Use of genetically modified muscle and fat grafts to repair defects in bone and cartilage. Eur Cell Mater 2009; **18**: 96–111.

14 Lee JY, Peng H, Usas A, Musgrave D, Cummins J, Pelinkovic D et al. Enhancement of bone healing based on ex vivo gene therapy using human muscle-derived cells expressing bone morphogenetic protein 2. Hum Gene Ther 2002; **13**: 1201–1211.

15 Musgrave DS, Pruchnic R, Bosch P, Ziran BH, Whalen J, Huard J. Human skeletal muscle cells in ex vivo gene therapy to deliver bone morphogenetic protein-2. J Bone Joint Surg Br 2002; **84**: 120–127.

16 Aslan H, Zilberman Y, Arbeli V, Sheyn D, Matan Y, Liebergall M et al. Nucleofection-based ex vivo nonviral gene delivery to human stem cells as a platform for tissue regeneration. Tissue Eng 2006; **12**: 877–889.

17 Miyazaki M, Zuk PA, Zou J, Yoon SH, Wei F, Morishita Y et al. Comparison of human mesenchymal stem cells derived from adipose tissue and bone marrow for ex vivo gene therapy in rat spinal fusion model. Spine (Phila PA 1976) 2008; **33**: 863–869.

18 Uludag H, D'Augusta D, Palmer R, Timony G, Wozney J. Characterization of rhBMP-2 pharmacokinetics implanted with biomaterial carriers in the rat ectopic model. J Biomed Mater Res 1999; **46**: 193–202.

19 Miyazaki M, Sugiyama O, Zou J, Yoon SH, Wei F, Morishita Y et al. Comparison of lentiviral and adenoviral gene therapy for spinal fusion in rats. Spine (Phila PA 1976) 2008; **33**: 1410–1417.

20 Feeley BT, Conduah AH, Sugiyama O, Krenek L, Chen IS, Lieberman JR. In vivo molecular imaging of adenoviral versus lentiviral gene therapy in two bone formation models. J Orthop Res 2006; **24**: 1709–1721.

21 Gamradt SC, Abe N, Bahamonde ME, Lee YP, Nelson SD, Lyons KM et al. Tracking expression of virally mediated BMP-2 in gene therapy for bone repair. Clin Orthop Relat Res 2006; **450**: 238–245.

22 Gazit D, Turgeman G, Kelley P, Wang E, Jalenak M, Zilberman Y et al. Engineered pluripotent mesenchymal cells integrate and differentiate in regenerating bone: a novel cell-mediated gene therapy. J Gene Med 1999; **1**: 121–133.

23 Koefoed M, Ito H, Gromov K, Reynolds DG, Awad HA, Rubery PT et al. Biological effects of rAAV-caAlk2 coating on structural allograft healing. Mol Ther 2005; **12**: 212–218.

24 Ito H, Koefoed M, Tiyapatanaputi P, Gromov K, Goater JJ, Carmouche J et al. Remodeling of cortical bone allografts mediated by adherent rAAV-RANKL and VEGF gene therapy. Nat Med 2005; 11: 291–297.

25 Repic D, Torreggiani E, Franceschetti T, Matthews BG, Ivcevic S, Lichtler AC et al. Utilization of transgenic models in the evaluation of osteogenic differentiation of embryonic stem cells. Connect Tissue Res 2013; 54: 296–304.

26 Bakhtina A, Tohfafarosh M, Lichtler A, Arinzeh TL. Characterization and differentiation potential of rabbit mesenchymal stem cells for translational regenerative medicine. In Vitro Cell Dev Biol Anim 2014; 50: 251–260.

27 Alaee F, Sugiyama O, Virk MS, Tang H, Drissi H, Lichtler AC et al. Suicide gene approach using a dual-expression lentiviral vector to enhance the safety of ex vivo gene therapy for bone repair. Gene Therapy 2014; 21: 139–147.

28 Kung SK, An DS, Chen IS. A murine leukemia virus (MuLV) long terminal repeat derived from rhesus macaques in the context of a lentivirus vector and MuLV gag sequence results in high-level gene expression in human T lymphocytes. J Virol 2000; 74: 3668–3681.

29 Sugiyama O, An DS, Kung SP, Feeley BT, Gamradt S, Liu NQ et al. Lentivirus-mediated gene transfer induces long-term transgene expression of BMP-2 in vitro and new bone formation in vivo. Mol Ther 2005; 11: 390–398.

30 Alaee F, Hong SH, Dukas AG, Pensak MJ, Rowe DW, Lieberman JR. Evaluation of osteogenic cell differentiation in response to bone morphogenetic protein or demineralized bone matrix in a critical sized defect model using GFP reporter mice. J Orthop Res 2014; 32: 1120–1128.

31 Jiang X, Kalajzic Z, Maye P, Braut A, Bellizzi J, Mina M et al. Histological analysis of GFP expression in murine bone. J Histochem Cytochem 2005; 53: 593–602.

32 Ushiku C, Adams DJ, Jiang X, Wang L, Rowe DW. Long bone fracture repair in mice harboring GFP reporters for cells within the osteoblastic lineage. J Orthop Res 2010; 28: 1338–1347.

33 Alaee F, Hong SH, Dukas AG, Pensak MJ, Rowe DW, Lieberman JR. Evaluation of osteoprogenitor cell response to bone morphogenetic protein and demineralized bone matrix in a critical sized defect model using GFP reporter mice. Orthopaedic Research Society Annual Meeting: San Antonio, TX, USA, 26–29 January 2013.

34 Hong SH JX, Chen L, Shin DG, Rowe D (eds). An update on automated 2D bone histomorphometry. XIIth Congress of the International Society of Bone Morphometry: Minneapolis, MN, USA, 16–19 October 2012.

35 Hong SH, Jiang X, Chen L, Josh P, Shin DG, Rowe D. Computer-automated static, dynamic and cellular bone histomorphometry. J Tissue Sci Eng 2012; (Suppl 1): 004.

36 Parfitt AM, Drezner MK, Glorieux FH, Kanis JA, Malluche H, Meunier PJ et al. Bone histomorphometry: standardization of nomenclature, symbols, and units. Report of the ASBMR Histomorphometry Nomenclature Committee. J Bone Miner Res 1987; 2: 595–610.

37 Otsu N. A threshold selection method from gray-scale histogram. IEEE Trans Systems, Man and Cybernetics 1978; 9: 62–66.